ACS APPLIED MATERIALS & INTERFACES

Research Article

www.acsami.org

Host–Guest Interaction-Based Self-Engineering of Nano-Sized Vesicles for Co-Delivery of Genes and Anticancer Drugs

Bin Yang, Xing Dong, Qi Lei, Renxi Zhuo, Jun Feng,* and Xianzheng Zhang

Key Laboratory of Biomedical Polymers (Ministry of Education), Department of Chemistry, Wuhan University, Wuhan 430072, P. R. China

ABSTRACT: On the basis of host–guest interactions, this study reported a kind of linear–hyperbranched supramolecular amphiphile and its assembled vesicles for the combined achievement of drug encapsulation and DNA delivery. Amine-attached β-cyclodextrin-centered hyperbranched polyglycerol and linear adamantane-terminated octadecane were arranged to spontaneously interlink together and then self-assemble into nanoscale vesicles. As the model of a hydrophilic agent, DOX·HCl was demonstrated to be readily loaded into the hollow cavity of the vesicles. The drug release pattern could be controlled by adjusting the environmental acidity, favoring the intracellularly fast drug liberation in response to the cellular lysosomal microenvironment. The nanovesicles displayed superior serum-tolerant transgene ability and significantly lower cytotoxicity compared to those of PEI25K, the gold standard of gene delivery vectors. The drug-loaded nanovesicle can co-deliver DNA payloads into cells and allow the preferable accumulation of two payloads in nuclei. The drug encapsulation was found to have little influence on the transfection. This co-delivery vehicle presents a good example of rational design of cationic supramolecular vesicles for stimulus-responsive drug/DNA transport.

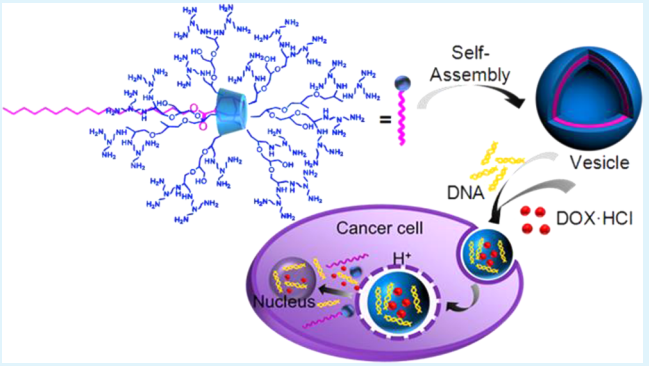

KEYWORDS: *nanovesicles, host–guest interaction, supramolecular assembly, drug encapsulation, gene delivery*

1. INTRODUCTION

One promising trend in developing highly efficient nanomedicines lies in the engineering of suitable nanoplatforms that can simultaneously accommodate multiple biofunctional species (e.g., therapeutic agents and diagnostic factors) and concurrently transport them into the host cells.[1−5] The integration of two or more different therapeutic mechanisms in one nanosystem can potentially produce synergistic effects and offer better treatment outcomes.[6−8] However, marked differences in the physicochemical properties exist among these biofunctional species, leading to great difficulties in the engineering of suitable codelivery nanosystems.[9−12] For instance, electrostatic condensation into nanocomplexes by cationic carriers has been acknowledged to be the most promising solution for the nonviral delivery of macromolecular genes, whereas small-molecule drugs have to be physically embedded into the nanoparticles (NPs) or conjugated to the carriers via chemically labile linkages.[13,14]

Because of the fast diffusion rate of small hydrophilic agents, their sustained delivery is difficult to achieve, and suitable delivery systems are currently largely unavailable. Vesicles not only can embed hydrophobic agents into the membranous layer but also can encapsulate hydrophilic agents inside the aqueous cavity, leading to their significant role in the field of sustained drug delivery.[15,16] Compared with liposome vesicles for drug delivery applications, polymeric vesicles displayed superior advantages, including good stability, easy surface functionalization (e.g., active targeting and fluorescent imaging),[17,18] and no usage of helper lipids.[19,20] However, controlling the liberation of entrapped payloads remains a significant challenge, which has to be addressed to overcome the low permeability of polymeric vesicles.[21,22] This predicament raises more rigorous demands on the carrier design for the codelivery of a gene and a small hydrophilic drug, and consequently, the studies in this field are very limited.[23−25]

Supramolecular chemistry provides great convenience and versatility in molecular design and the expansion of its function. The inclusion complexation between cyclodextrin (CD) and various guests has been extensively investigated in supramolecular chemistry.[26,27] CD has been frequently chemically conjugated to the materials for improved water solubility and biocompatibility. In addition, CD can readily undergo chemical modification for the acquisition of desired functions. Taking advantage of host–guest chemistry, we report the supramolecular engineering of a polymeric nanovesicle for the controlled codelivery of plasmid DNA and hydrophilic drugs. Tris(2-aminoethyl)amine-attached β-cyclodextrin-centered hyperbranched polyglycerol (CD-HPG-TAEA) and linear ada-

Received: August 14, 2015
Accepted: September 15, 2015
Published: September 23, 2015

DOI: 10.1021/acsami.5b07549
ACS Appl. Mater. Interfaces 2015, 7, 22084–22094

mantane-terminated octadecane (C_{18}-AD) were arranged to interlink together, leading to the supramolecular amphiphilic conjugate used as the building units for nanovesicle engineering (Scheme 1). This amine-rich nanovesicle can entrap hydrophilic drugs and simultaneously bind with positively charged plasmid DNA, allowing the concurrent cellular internalization of two payloads with high efficiency. It is known that liposome delivery vesicles commonly need helper lipids such as dioleoylphosphatidylethanolamine (DOPE) to facilitate membrane fusion and the destabilization of the endosome.[28,29] Compared with it, the enrichment of multivalent amine groups within the designed nanovesicle ensures the effective endosomal escape due to the well-established proton sponge effect.[30,31] In addition, the amine protonation upon entry into a gradually acidified endosome would enhance both the hydrophilicity and the charge repulsion of vesicle-forming units. This would weaken the compactness of the vesicular membrane and make the membrane leaky to the encapsulated drugs, benefiting the effective drug release inside cells. This paradigm established on the host−guest interaction provides great chances to extend the functions by partially changing the guest molecules, e.g., using bioimaging molecules.

Scheme 1. Illustration of Nanovesicle Self-Engineering Driven by Host−Guest Interaction between AD-C_{18} and CD-HPG-TAEA for Gene Delivery and Drug Encapsulation

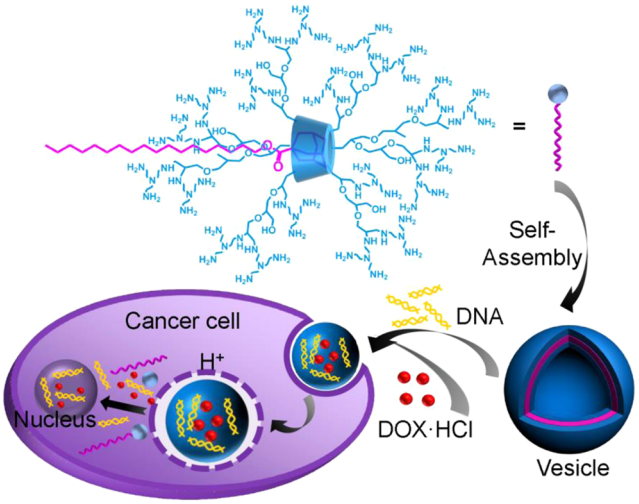

2. EXPERIMENTAL SECTION

Materials. Tetrahydrofuran (THF, Shanghai Chemical Reagent Ltd.) was purified by being distilled over Na with benzophenone as the color indicator. *N*,*N*-Dimethylformamide (DMF, Shanghai Chemical Reagent Ltd.) and dimethyl sulfoxide (DMSO, Shanghai Chemical Reagent Ltd.) were distilled over CaH_2 under reduced pressure. Glycidol (96%, Sigma) was distilled under reduced pressure before being used. Potassium hydride (25−35 wt %, dispersion in mineral oil, Alfa) was washed with dry tetrahydrofuran and then dried in vacuum. *β*-Cyclodextrin (*β*-CD), 18-crown-6 ether, *N*,*N*′-carbonyldiimidazole (CDI), 1-adamantanecarbonyl chloride, 1-octadecanol, and tris(2-aminoethyl)amine (TAEA) were used as received (J&K Chemical Ltd.). Doxorubicin hydrochloride (DOX·HCl) was purchased from Zhejiang Hisun Pharmaceutical Co., Ltd., and other chemicals were purchased from Shanghai Chemical Reagent Ltd. and used without any treatments.

Dulbecco's modified Eagle's Medium (DMEM), fetal bovine serum (FBS), phosphate-buffered saline (PBS), penicillin streptomycin, trypsin, and 3-(4,5-dimethylthiazol-2-yl)-2,5-diphenyltetrazolium bromide (MTT) were purchased from Invitrogen Corp.

Synthesis of Hyperbranched Polyglycerol Grafted from *β*-Cyclodextrin (CD-HPG). CD-HPG was synthesized by the anionic ring opening polymerization according to the method described in ref 32. *β*-Cyclodextrin (0.4 g, 0.352 mmol) and 18-crown-6 ether (0.66 g, 2.5 mmol) were dissolved in DMF (15 mL) and added to a 50 mL flask with potassium hydride (0.112 g, 2.8 mmol). After being stirred for 2 h at 50 °C, the mixture was warmed to 80 °C, and a glycidol (2.0 g, 25.8 mmol; 1.0 g, 12.9 mmol) solution in DMF (10 mL) was introduced slowly into the system over 24 h. The reaction mixture was then dialyzed against distilled water [molecular weight cutoff (MWCO) of 3500] for 5 days. After that, the sample was lyophilized to give the transparent and viscous liquid product. Via adjustment of the ratio of glycidol to CD in feed, two polymers were obtained and denoted as CD-HPG_{36} and CD-HPG_{17}, respectively (where 36 and 17 refer to the number of glycidols grafted from CD).

Synthesis of Amine-Attached *β*-Cyclodextrin-Centered Hyperbranched Polyglycerol (CD-HPG-TAEA). CD-HPG-TAEA was prepared by a modification of the procedure described in the literature.[33,34] Typically, to a solution of CDI (3.1 g, 19 mmol) in DMF (10 mL) was added dropwise CD-HPG_{36} (1.0 g, 9.5 mmol hydroxyl groups) in DMF (10 mL) over 1 h while the mixture was being stirred. After reaction for 2 h, the solution was poured into a large amount of Et_2O. The precipitate was isolated by centrifugation and further washed thrice with Et_2O. Then the precipitate was dissolved in anhydrous DMSO (15 mL). Triethylamine (TEA) (1 mL) was mixed with the as-prepared solution and then added dropwise to a solution of TAEA (2.8 g, 19 mmol) in DMSO (5 mL) over 1 h. After 24 h, the reaction solution was dialyzed (MWCO of 3500) against water for 3 days. The dialyzate was freeze-dried to yield pale yellow solids. Via this method, two polymers were obtained and denoted as CD-HPG_{36}-$TAEA_{30}$ and CD-HPG_{17}-$TAEA_{13}$ (where 30 and 13 refer to the number of TAEA groups).

Synthesis of the Adamantane-Terminated Alkyl Chain (C_{18}-AD). The synthesis of C_{18}-AD was based on the esterification reaction between octadecanol and adamantanecarbonyl chloride. At 0 °C, 1-adamantanecarbonyl chloride (1 g, 5.04 mmol) in dried THF (10 mL) was dropwise added to the solution of 1-octadecanol (1.65 g, 6.1 mmol) and triethylamine (0.85 mL, 6.1 mmol) in dried THF (30 mL) over 30 min under a N_2 atmosphere. Then the mixture was warmed to room temperature and reacted overnight. A crude product of white solid was obtained after the salt of triethylammonium chloride had been isolated and the solvent removed via rotation evaporation. The product was purified by column chromatography on silica gel (1/8 CH_2Cl_2/hexane) to give C_{18}-AD as a white solid.

Construction of Supramolecular C_{18}-AD/CD-HPG-TAEA Nanovesicles. Typically, CD-HPG_{36}-$TAEA_{30}$ (135 mg, 0.015 mmol) and C_{18}-AD (10 mg, 0.023 mmol) were dissolved together in 5 mL of DMF at 50 °C and stirred for 1 h. Subsequently, 2 mL of water was slowly added within 2 h. The solution became slightly blue, indicating the occurrence of self-assembly. After being stirred overnight at 50 °C, the solution was dialyzed (MWCO of 3500) against water for 3 days to remove DMF. The dialyzate was filtered and freeze-dried to provide the supramolecular C_{18}-AD/CD-HPG_{36}-$TAEA_{30}$ assemblies.

Characterizations. ^1H nuclear magnetic resonance (NMR) and ^{13}C NMR spectra were recorded (Varian Unity 300 MHz spectrometer) in $CDCl_3$ or D_2O, and tetramethylsilane (TMS) served as the internal standard. The molecular weight (M_w) and polydispersity index (PDI) of polymers were measured by a size-exclusion chromatography and multiangle laser light scattering (SEC-MALLS) instrument equipped with a dual-detector system consisting of a MALLS device (DAWNEOS, Wyatt Technology) and an interferometric refractometer (Optilab DSP, Wyatt Technology). A 0.1 M $NaNO_3$ solution and a 0.1 M HAc/NaAc (pH 4.2) buffer solution were used as the eluent at a flow rate of 0.3 mL/min. The MALLS detector was operated at a laser wavelength of 690.0 nm. The hydrodynamic diameters of C_{18}-AD/CD-HPG-TAEA assemblies were determined by dynamic light scattering (DLS) measurements at 25 °C

DOI: 10.1021/acsami.5b07549
ACS Appl. Mater. Interfaces 2015, 7, 22084−22094

(Malvern Zetasizer Nano-ZS ZEN3600 equipped with a 4 mW He−Ne laser). Transmission electron microscopy was performed on a FEI Tecnai G^2 20 TWIN instrument with an acceleration voltage of 200 kV. The samples were prepared by dipping a copper Ttransmission electron microscopy grid into the assembly solution and then drying them in air.

Cell Culture and Amplification of Plasmid DNA. African green monkey SV40-transformed kidney fibroblast (COS7) cells and human breast adenocarcinoma (MCF-7) cells were incubated at 37 °C in DMEM containing 10% FBS and 1% antibiotics (penicillin-streptomycin, 10000 units/mL) in a humidified atmosphere containing 5% CO_2.

As the luciferase reporter gene, plasmid pGL-3 was transformed in *Escherichia coli* JM109 and amplified in terrific broth medium at 37 °C overnight at 250 rpm. After the treatment with an EndoFree QiAfilter Plasmid Giga Kit (5) (QIAGEN), the purified plasmid was dissolved in a TE buffer solution and stored at −20 °C. The integrity of plasmid was validated by agarose gel electrophoresis. The concentration and purity of the plasmid were measured on the basis of the ultraviolet (UV) absorbance obtained at 260 and 280 nm, respectively.

Agarose Gel Retardation Assay. The vector/DNA complexes were prepared at different N/P ratios, using 0.5 μL of pGL-3 DNA (200 ng/μL). All the complex solutions were diluted with a 150 mM NaCl solution to a total volume of 8 μL and then incubated at 37 °C for 0.5 h. After that, the complexes were electrophoresed on the 0.7% (w/v) agarose gel containing GelRed using Tris-acetate (TAE) running buffer at 80 V for 60 min. The migration of DNA was visualized and photographed on a UV lamp using a Vilber Lourmat imaging system.

Particle Size and ζ Potential of Complexes. The hydrodynamic diameter and ζ potential of the obtained complexes were determined by DLS at 173° scattering. Using a method similar to that described above, the solutions of vector/DNA complexes prepared in 10 mM phosphate buffer (pH 7.4) were vortexed for 10 s and incubated for 30 min at 37 °C prior to the measurement of hydrodynamic diameter. For ζ potential measurement, ultrapure water was used as the solvent.

Cytotoxicity Assay. The *in vitro* cytotoxicity assay was tested in COS7 and MCF-7 cells by the MTT method. Briefly, 100 μL of the cell suspension with a density of 60 cells/μL was plated into 96-well plates and subjected to a 24 h incubation in 100 μL of DMEM containing 10% FBS. The samples with different concentrations were then added to each well. After a 4 h co-incubation, the medium was replaced with 200 μL of fresh medium and continually cultured for 44 h. After a further 4 h incubation following the addition of 20 μL of MTT (5 mg/mL), the medium was aspirated and the MTT-formazan generated by live cells was dissolved in 150 μL of DMSO. The optical density (OD) of the medium was measured by a microplate reader (Bio-Rad, model 550) at 570 nm. The relative cell viability (RCV) was defined as RCV (%) = $(OD_{samples} - OD_{background})/(OD_{control} - OD_{background}) \times 100$, where OD_{sample} and $OD_{control}$ were measured in the presence and absence of samples. Data are shown as means ± the standard deviation (SD) on the basis of independent experiments.

Transfection Study by the Luciferase Assay. The *in vitro* transfections mediated by the plasmid pGL-3-containing complexes were conducted in COS7 and MCF-7 cells at 37 °C, using PEI25K complexes as the positive control prepared at the optimal N/P ratio. Cells (6×10^4 cells/well) were seeded in 24-well plates and cultured with 1 mL of DMEM containing 10% FBS for 24 h. Then the culture media were replaced with the complex solution in serum-free or 10% FBS-containing DMEM (1 mL). After a 4 h co-incubation and subsequent removal of the medium, the cells were further cultured in fresh 10% FBS containing DMEM for 44 h. Then the isolated cells were washed with 0.25 mL of PBS, and the luciferase assay was performed. The relative light units (RLUs) were determined on a chemiluminometer (Lumat LB9507, EG&G Berthold). On the basis of the obtained data about the total amount of protein according to a BCA protein assay kit (Pierce), the luciferase activity (RLU/mg of protein) was acquired.

Confocal Laser Scanning Microscopy (CLSM). The ability of the vecors to transport DNAs and DOX·HCl into cells was investigated by CLSM. COS7 cells (1×10^5 cells/well) were seeded in a single dish and cultured for 24 h. One microgram of pGL-3 DNA was labeled with 2.5 μL of 10 mM YOYO-1 at 37 °C for 15 min prior to the observation. The polyplexes prepared with the empty and drug-loaded vesicles were incubated for 30 min and subsequently introduced into the dishes. After co-incubation for 4 h for drug-free polyplexes and 8 h for drug-loaded polyplexes, the media were removed and the cells were repeatedly washed with PBS. Following the 15 min exposure to 10 μL (2 μg/μL) of Hoechst 33342 for staining of nuclei, the cells were washed with PBS repeatedly and introduced into 1 mL of DMEM for CLSM observation (C1-Si, Nikon). The fluorescence originating from Hoechst 33342, YOYO-1, and DOX was excited at 405, 488, and 543 nm, respectively.

Flow Cytometry. Flow cytometry was employed to quantify the cellular uptake efficiency of the vectors. COS7 cells (5×10^4 cells/well) were seeded in 24-well plates and cultured with 1 mL of 10% FBS containing DMEM for 24 h. The polyplexes of YOYO-1-stained pGL-3 (1 μg) were prepared at their optimal N/P ratios in 100 μL of PBS and then diluted to 1 mL by adding 900 μL of serum-free DMEM. Following a 4 h cell incubation with the polyplexes, the media were withdrawn. The remaining cells were washed thrice with PBS and digested with trypsin. Subsequently, the cells were collected by centrifugation at 1000 rpm for 5 min. The bottom cells were washed twice with pH ∼7.4 PBS. Then the suspended cells were filtered and analyzed by flow cytometry (BD FACSAria III). The instrument was calibrated using nontransfected cells, and the transfected cells were examined from a fluorescence scan performed with 1×10^4 cells using the FL1-H channel.

Drug Loading and pH-Dependent Release. The process of loading a drug in C_{18}-AD/CD-HPG_{36}-$TAEA_{30}$ assemblies can be briefly described as follows.[35] DOX·HCl (10 mg) was mixed with C_{18}-AD/CD-HPG_{36}-$TAEA_{30}$ (30 mg) in 5 mL of DMSO overnight and then dialyzed against deionized water (2 L) using a regenerated cellulose acetate membrane (MWCO of 3500) for 24 h to remove DMF and unloaded DOX·HCl. During the process, the dialyzate was replaced every 6 h. After that, the solution was lyophilized to obtain the drug-loaded samples. The loading amount of DOX·HCl in the assemblies was determined according to the UV absorbance intensity measured at 485 nm in a DMF solution, using an experimentally obtained standard calibration curve. The drug loading efficiency (DLE) is calculated with the equation DLE (%) = (mass of drug loaded/mass of drug-loaded nanoassemblies) × 100%.

In vitro release behaviors of DOX·HCl from C_{18}-AD/CD-HPG_{36}-$TAEA_{30}$ assemblies were studied under different pH conditions. First, drug-loaded assemblies were dissolved in deionized water (1 mg/mL) and transferred into the dialysis membrane tube (MWCO of 3500). The tube was immersed in 10 mL of a 0.01 M acetate buffer solution (pH 5.0) and 0.01 M phosphate-buffered saline (pH 7.4) while being shaken at 37 °C. At the predetermined intervals, the external buffer was withdrawn and the same volume of fresh buffer was introduced. The amount of released DOX·HCl was determined by measuring the DOX·HCl concentration in the external buffer using an RF-5301PC spectrofluorophotometer (Shimadzu), using an experimentally obtained standard calibration curve. The excitation wavelength was set at 488 nm, and the spectra were recorded over the emission range from 500 to 650 nm. The initial mass of loaded drug was determined on the basis of the as-obtained DLE.

Transfection with Drug-Loaded Polyplexes. To investigate the influence of drug loading on transfection, C_{18}-AD/CD-HPG_{36}-$TAEA_{30}$/DNA/DOX·HCl polyplexes were also subjected to the luciferase assay in the same manner as mentioned above. The polyplexes were prepared at N/P ratios of 30, 40, and 50.

3. RESULTS AND DISCUSSION

Preparation and Characterization of Supermolecular Nanovesicles. Vesicle formation relied on the self-assembly of the supramolecular conjugate between tris(2-aminoethyl)-amine-attached β-cyclodextrin-centered hyperbranched polyglycerol (CD-HPG-TAEA) and linear adamantane-terminated

DOI: 10.1021/acsami.5b07549
ACS Appl. Mater. Interfaces 2015, 7, 22084−22094

Scheme 2. Synthesis Routes of (A) CD-HPG-TAEA and (B) C_{18}-AD

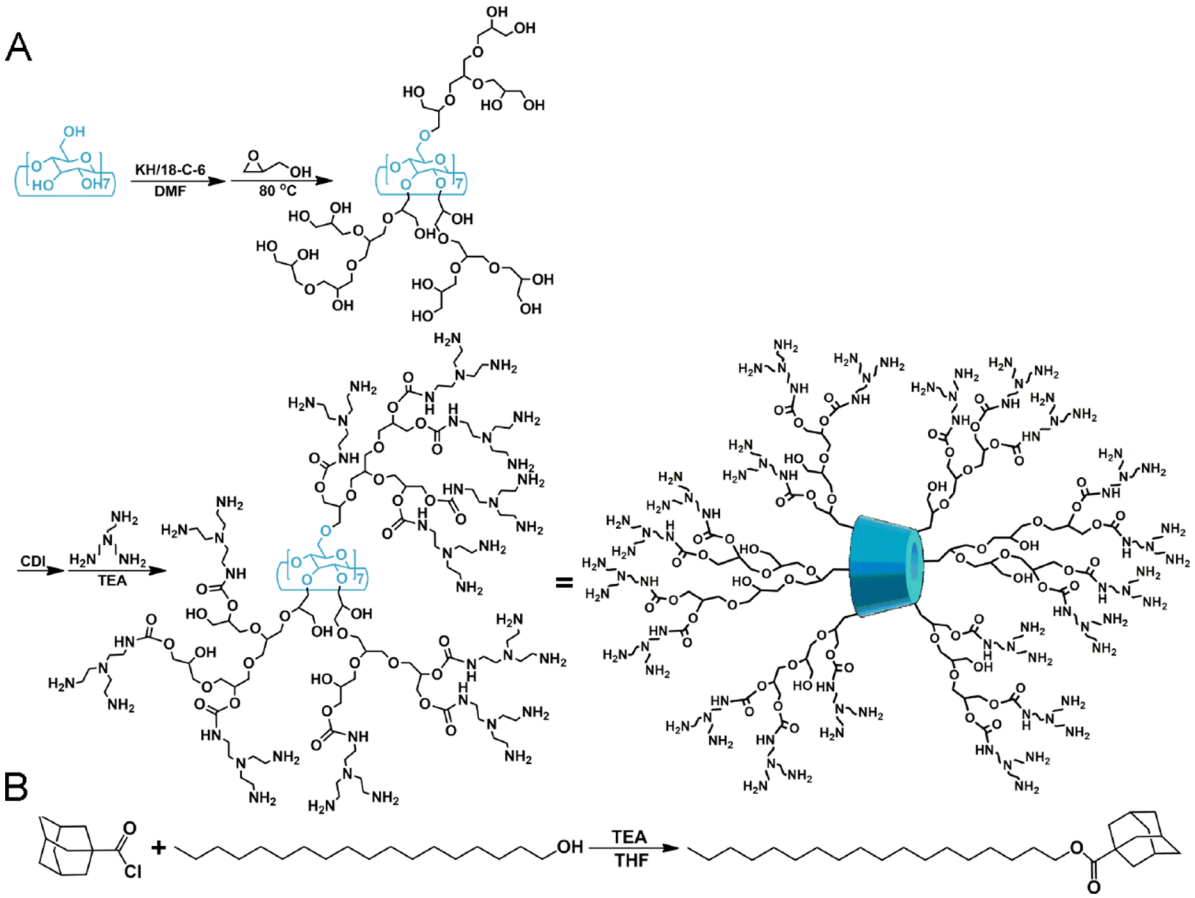

octadecane (C_{18}-AD) driven by the host−guest interaction. As shown in Scheme 2, the chemical attachment of hyperbranched glycerol (HPG) surrounding β-cyclodextrin (β-CD) was accomplished by anionic ring-opening multibranching polymerization of glycidol using β-CD as the core initiator in the presence of 18-crown-6 ether and potassium hydride. Tris(2-aminoethyl)amine (TAEA) was further chemically connected to the hyperbranched CD-HPG by the CDI method. The products were purified by the dialysis treatment. Hydrophobic C_{18}-AD was synthesized through the esterification reaction of octadecanol with adamantanecarbonyl chloride.

The structures of all the products were verified by NMR spectroanalyses. In the ^{1}H NMR spectrum of CD-HPG (Figure 1B), the proton signals belonging to the HPG segment at 4.2−3.3 ppm with strong intensities were overlapped with those attributed to H2−H6 protons of CD. Meanwhile, the H1 signal of CD was shifted to lower field after the reaction. The ^{13}C NMR spectrum of CD-HPG disclosed the definite structure of the hyperbranched HPG segment, including the linear, dendritic, and terminal units (Figure 1E). In addition, the resonance occurring at 101 ppm was attributed to C1 of the CD group. The degree of polymerization (DP) of HPG can be calculated on the basis of the ^{1}H NMR spectrum using a similar method reported in ref 32. After the reaction with TAEA, new signals emerged in the range of 3.2−3.0 ppm (-CONHCH_2-) and 2.9−2.3 ppm (-CH_2CH_2NH_2), indicating the successful synthesis of CD-HPG-TAEA (Figure 1C). The actual degree of grafting of TAEA was determined by comparing the signal integrals of HPG and TAEA.[36] Consequently, two polymers denoted as CD-HPG$_{36}$-TAEA$_{30}$ and CD-HPG$_{17}$-TAEA$_{13}$ (the subscripts refer to the number of HPG repeat units and TAEA number per polymer molecule, respectively) were studied and had approximate ratio values of HPG repeat units versus TAEA.

The SEC-MALLS technique was applied to give the molecular weights [$M_{n(SEC)}$] of CD-HPG-TAEA polymers. All the data, including the $M_{n(SEC)}$ and $M_{n(HNMR)}$ values calculated according to ^{1}H NMR spectra, are listed in Table 1. Relative to $M_{n(HNMR)}$, a higher $M_{n(SEC)}$ was obtained for all the polymers with a moderate polydispersity. This may be ascribed to the special hyperbranched architecture of CD-HPG-TAEA and the cause originating from different measurements.

Like amphiphilic copolymers, the C_{18}-AD/CD-HPG-TAEA conjugate intended to assemble into the microphase-separated aggregates that are well-dispersed in aqueous media. The morphology of the obtained aggregates can be inspected by a transmission electron microscope (TEM), which is a commonly used tool for examining the vesicular morphology. As shown in panels A and B of Figure 2, neat vesicles ~200 nm in size were formed and uniformly distributed for both C_{18}-AD/CD-HPG$_{36}$-TAEA$_{30}$ and C_{18}-AD/CD-HPG$_{17}$-TAEA$_{13}$ conjugates. The former appeared to have a thinner membrane layer, indicating the relatively looser structure resulting from the stronger charge repulsion among the vesicle-forming units. The two conjugates had similar hydrodynamic diameters of ~310 nm determined by dynamic light scattering (DLS). Relative to the size measured by the TEM, the larger DLS diameter was mainly due to the dry state of the nanovesicles during TEM observation. The assembly diameter remained almost steady in solution at 25 °C over 2 weeks, indicative of good stability. The ζ potentials of C_{18}-AD/CD-HPG$_{36}$-TAEA$_{30}$

DOI: 10.1021/acsami.5b07549
ACS Appl. Mater. Interfaces 2015, 7, 22084−22094

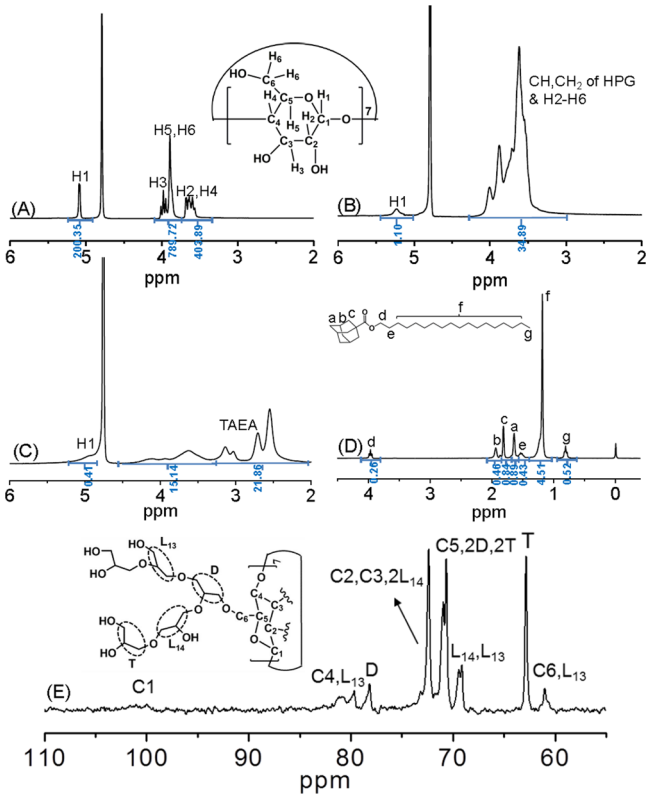

Figure 1. ^{1}H NMR spectra of (A) CD, (B) CD-HPG$_{36}$, and (C) CD-HPG$_{36}$-TAEA$_{30}$ in D_2O and (D) C_{18}-AD in $CDCl_3$. (E) ^{13}C NMR spectrum of CD-HPG$_{36}$ in D_2O (L, linear; T, terminal; D, dendritic).

Table 1. Results of CD-HPGs and CD-HPG-TAEAs

sample	M_n [a]	M_n [b]	PDI [b]
CD-HPG$_{36}$	3800	5800	1.40
CD-HPG$_{17}$	2400	3900	1.06
CD-HPG$_{36}$-TAEA$_{30}$	8960	14600	1.56
CD-HPG$_{17}$-TAEA$_{13}$	4630	7500	1.38

[a]Determined by ^{1}H NMR. [b]Determined by SEC-MALLS using a 0.1 M $NaNO_3$ solution as the eluent for CD-HPGs and a 0.1 M HAc/NaAc (pH 4.2) buffer solution for CD-HPG-TAEAs.

and C_{18}-AD/CD-HPG$_{17}$-TAEA$_{13}$ conjugates were determined to be 30.1 and 28.4 mV, respectively, by DLS. The higher potential of the former can be explained by the higher density of amine groups.

DNA Condensation. The capability of combining DNA is a fundamental requisite for DNA delivery vectors. The agarose gel retardation assay was applied to investigate the DNA affinity of the nanovesicles. As shown in Figure 3A–D, raw CD-HPG-TAEAs can entirely retard the migration of DNA starting from a lower N/P ratio of 4, while that occurred at a N/P ratio of 6 for corresponding C_{18}-AD/CD-HPG-TAEA vesicles. In most cases, the assembly of amphiphilic cationic polymers into solid micelles would more or less improve the electrostatic affinity for DNA.[37] This is mainly due to the fact that within the micellar structure, the cationic segment was compactly condensed as the shell to surround the hydrophobic core, which differed sharply from the free polycations. The resulting high charge density of nanomicelles would strengthen the electrostatic interaction with DNA. On the other hand, the weakened capability of DNA capture detected herein ought to

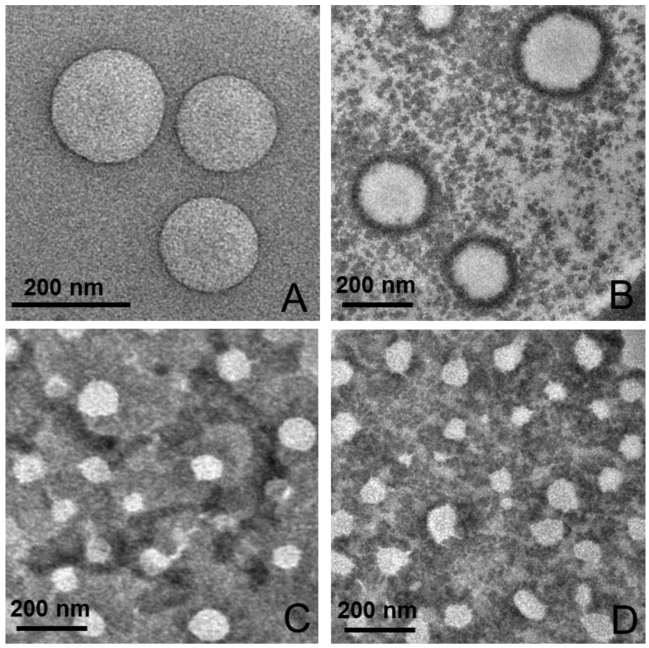

Figure 2. TEM images of (A) C_{18}-AD/CD-HPG$_{36}$-TAEA$_{30}$, (B) C_{18}-AD/CD-HPG$_{17}$-TAEA$_{13}$ vesicles, (C) C_{18}-AD/CD-HPG$_{36}$-TAEA$_{30}$/pGL-3, and (D) C_{18}-AD/CD-HPG$_{17}$-TAEA$_{13}$/pGL-3 complexes prepared at a N/P ratio of 50.

relate to the special hollow architecture of C_{18}-AD/CD-HPG-TAEA vesicles.

The surface potential and hydrodynamic diameter of DNA/vector nanocomplexes may affect their cellular internalization. The positively charged nanoparticles with diameters of <200 nm are documented to be suitable for the efficient cellular entry and passive accumulation in tumor tissues.[38,39] As shown in Figure 3F, with the increase in N/P ratios, the ζ potential displayed a gradual increment and then remained steady within a narrow range of 35–42 mV. This tendency appeared to hold true for the variation of hydrodynamic diameter, which fluctuated within the range from 100 to 210 nm (Figure 3E). Next, the complex morphology was observed by the TEM (Figure 2C,D). After binding with DNA, compact nanoparticles <100 nm in size were formed.[25]

***In Vitro* Cell Viability.** Low toxicity is required for synthetic delivery vehicles. The cell-toxic effects of the samples in tumorous MCF-7 cells and normal COS7 cells were tested by the MTT assay. PEI25K possesses high transfection activity and therefore is commonly used as the gold standard for the evaluation of nonviral gene vectors. However, its serious damage to cells impedes the practical applications. As shown in Figure 4, all the prepared samples exhibited cell safety apparently better than that of PEI25K. As expected, CD-HPG$_{36}$-TAEA$_{30}$ displayed stronger inhibition toward cell proliferation than CD-HPG$_{17}$-TAEA$_{13}$ because of the higher charge density of the former. The host–guest conjugation with C_{18}-AD led to the considerable reduction of the cell-toxic effect for both CD-HPG-TAEAs in the two cell lines. This result sounds reasonable when considering the reduced binding ability with DNAs after insertion of C_{18}-AD into CD-HPG-TAEAs. The weakened affinity for DNAs would result in less damage to the cell membranes.

Cellular Uptake. The ability of the vectors to deliver the entrapped DNA into host cells is one of the important factors

DOI: 10.1021/acsami.5b07549
ACS Appl. Mater. Interfaces 2015, 7, 22084–22094

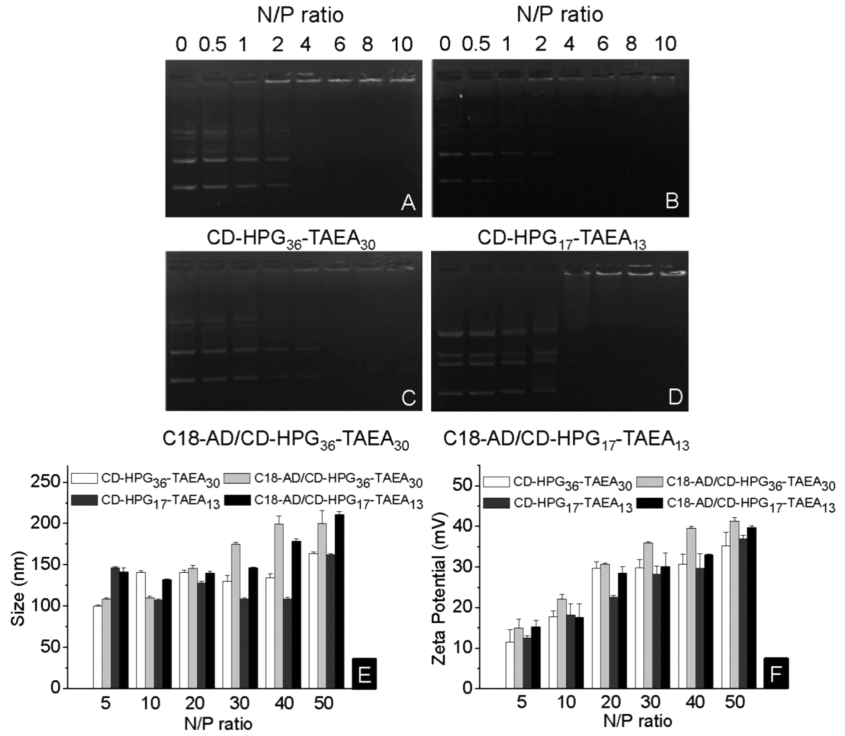

Figure 3. Agarose gel electrophoreses of (A and B) CD-HPG-TAEA and (C and D) C_{18}-AD/CD-HPG-TAEA complexes prepared at different N/P ratios. (E) Diameters and (F) ζ potentials of pGL-3/vectors complexes with different N/P ratios. Data are shown as means ± SD (n = 3).

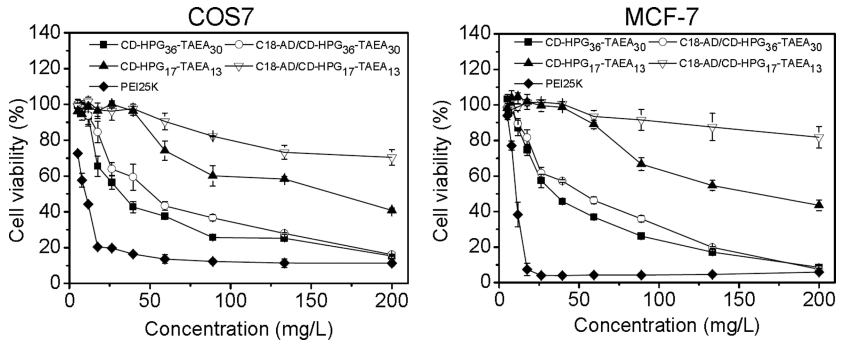

Figure 4. Cell viabilities of vectors and PEI25K in COS7 and MCF-7 cells. Data are means ± SD (n = 4).

affecting transfection efficacy. A confocal laser scanning microscope (CLSM) was applied to investigate the cellular internalization of vector/DNA complexes. As shown in Figure 5, all the vectors can effectively mediate the intracellular transport of the carried plasmid pGL-3. The green YOYO-1-labeled pGL-3 was mainly distributed in the cytoplasm domain after a 4 h co-incubation. In terms of the fluorescence intensity inside cells, CD-HPG$_{36}$-TAEA$_{30}$ and its inclusion assembly displayed transport capability stronger than that of the corresponding CD-HPG$_{17}$-TAEA$_{13}$ counterparts. This result was associated with the higher surface potential of the former because the electrostatic interaction was the main driving force accounting for the cellular access. As indicated from the CLSM observation, it seemed that the host−guest inclusion of C_{18}-AD into CD-HPG-TAEA had an insignificant influence on the delivery ability.

Flow cytometry provided quantitative data about the endocytosis efficiency (Figure 6). The best outcome of endocytosis rate (75.1%) was detected for CD-HPG$_{36}$-TAEA$_{30}$, which was even superior to the positive control of PEI25K (65.8%). Unlike CLSM observation, the obtained data indicated that the assembly with C_{18}-AD would impair the endocytosis efficiency by 17 and 21% for CD-HPG$_{36}$-TAEA$_{30}$ and CD-HPG$_{17}$-TAEA$_{13}$, respectively. The higher the amine density within the polymer, the weaker this tendency toward decline. This finding can be explained by the better ability of CD-HPG$_{36}$-TAEA$_{30}$ in mediating the cellular uptake. Consequently, the influence caused by C_{18}-AD inclusion was represented less profoundly.

***In Vitro* Transfection.** The *in vitro* transfection assays were conducted in COS7 and MCF-7 cells in the absence or presence of 10% serum. PEI25K was used as the positive control. As shown in panels A and B of Figure 7, CD-HPG$_{36}$-TAEA$_{30}$ and its assembly with C_{18}-AD exhibited transfection activities better than those of the corresponding CD-HPG$_{17}$-TAEA$_{13}$ counterparts in both cell lines. This correlated well with the higher cellular entry efficiency of the former. With respect to the transfection activity, the CD-HPG$_{36}$-TAEA$_{30}$/C_{18}-AD nanovesicle can even compete with PEI25K. Nevertheless, in contrast to the tendency of endocytosis efficiency,

DOI: 10.1021/acsami.5b07549
ACS Appl. Mater. Interfaces 2015, 7, 22084−22094

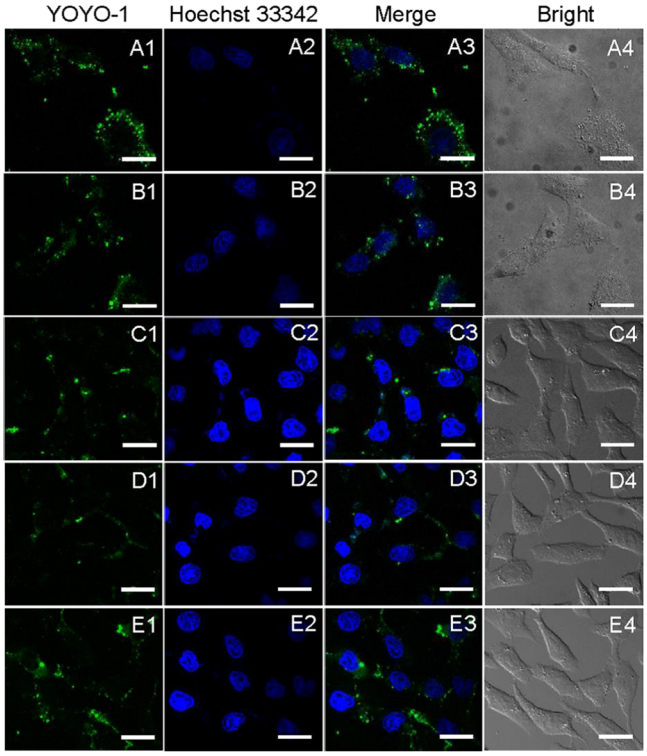

Figure 5. Confocal images of COS7 cells after a 4 h co-incubation with vector/DNA complexes prepared at the optimal transfection N/P ratios: (A) CD-HPG$_{36}$-TAEA$_{30}$, (B) C$_{18}$-AD/CD-HPG$_{36}$-TAEA$_{30}$, (C) CD-HPG$_{17}$-TAEA$_{13}$, (D) C$_{18}$-AD/CD-HPG$_{17}$-TAEA$_{13}$, and (E) PEI25K. Plasmid pGL-3 was stained green by YOYO-1. Nuclei of cells were stained blue by Hoechst 33342. Scale bars are 20 μm.

the inclusion of C$_{18}$-AD into CD-HPG-TAEA led to little variation and even a slight enhancement of the protein expression level. The results suggested that cellular entry may not be the sole factor determining the transfection performance.

The negatively charged components in the bloodstream would adsorb onto the polycations and thus cause the aggregation and/or sedimentation of polycation/DNA complexes, leading to the sacrifice of carried DNA payloads.[40,41] The serum-conditioned transfection has thus been a fundamental model used for the predictive evaluation on *in vivo* transfection. Therefore, the transfection assays were further conducted in the presence of 10% serum. As shown in panels C and D of Figure 7, the serum-conditioned transfection efficiencies mediated by the prepared vectors remained at a similar level in COS7 cells and had a small reduction in MCF-7 cells as compared with the serum-free controls. In comparison, the transfection efficiency of PEI25K was dramatically reduced by 18-fold in MCF-7 cells. The results suggested that the vectors including CD-HPG-TAEAs and their assemblies can effectively resist the serum-associated transfection inhibition. Our previous work had reported that the hydroxylation modification toward polycations can help prevent the complexes from the serum-caused aggregation and thus inhibit the downregulation of transfection efficiency.[42] Therefore, the result is thought to be associated with the enrichment of hydroxyl groups within HPG.

Drug Loading and pH-Dependent Release. Red fluorescent DOX·HCl frequently serves as the model of hydrophilic drugs and thus is used herein.[43,44] The formation of C$_{18}$-AD/CD-HPG$_{36}$-TAEA$_{30}$ nanovesicles and drug encapsulation into the hollow cavity were achieved through the dialysis method. The drug loading content was determined to

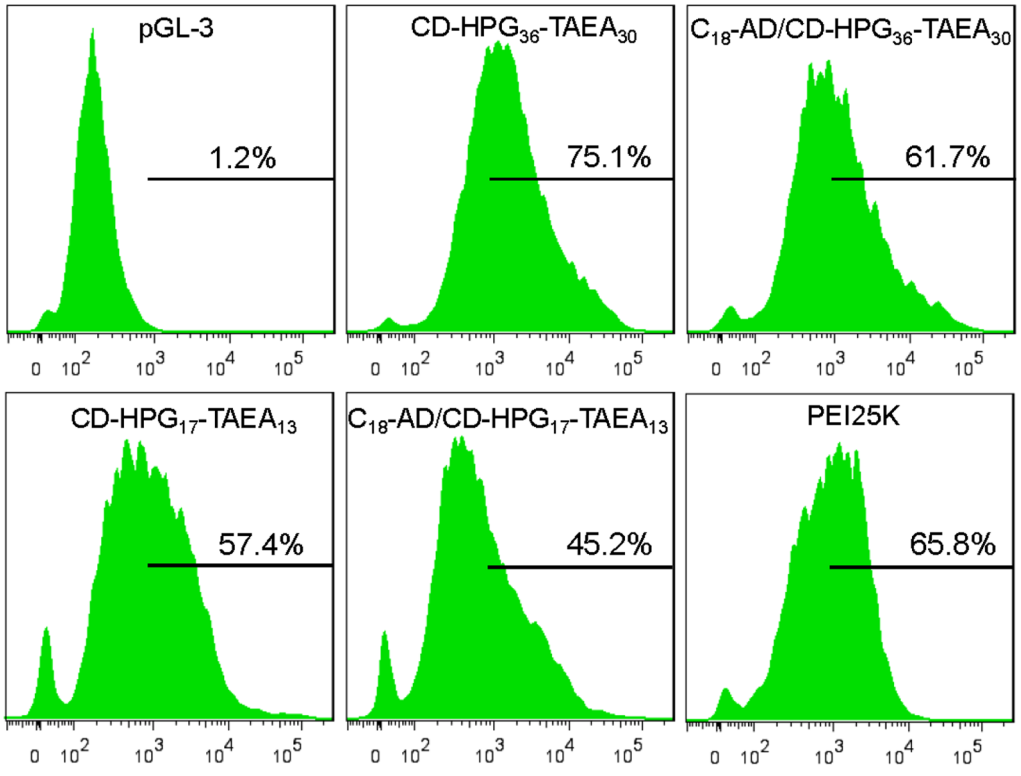

Figure 6. Flow cytometry profiles of naked pGL-3 and vector/pGL-3 complexes at their respective optimal transfection N/P ratios.

DOI: 10.1021/acsami.5b07549
ACS Appl. Mater. Interfaces 2015, 7, 22084−22094

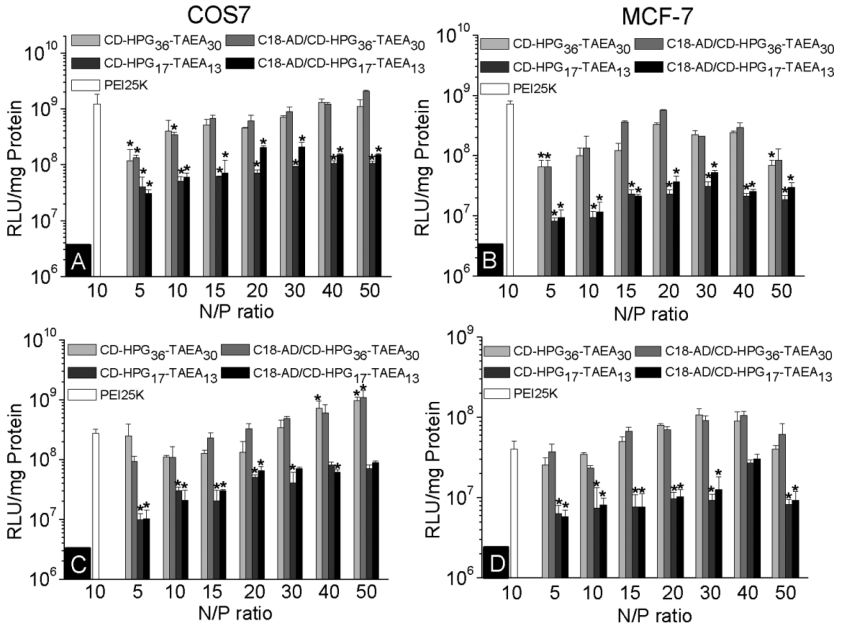

Figure 7. Transfection efficiencies of vector/DNA complexes prepared at various N/P ratios in the absence (A and B) and presence (C and D) of 10% serum in COS7 and MCF-7 cells. PEI25K was used as the positive control. Data are means ± SD (n = 3) (*p < 0.05 as compared with the data of PEI25K).

be 7.1%. The TEM image of the drug-encapsulated nanovesicle showed the appearance of dark areas in the hollow cavity (Figure 8A), suggesting that the drug was mostly loaded in the cavity.[45] The hydrodynamic diameter after drug loading underwent a slight increase from 310 to 340 nm.

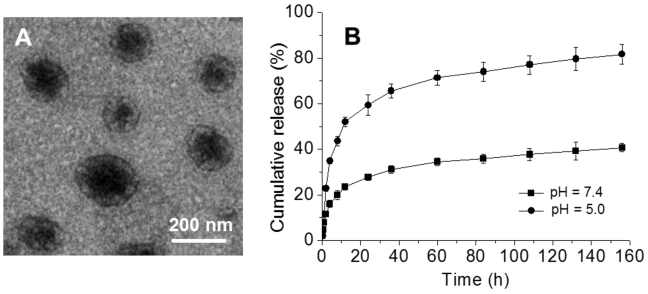

Figure 8. (A) TEM images of DOX·HCl-loaded C_{18}-AD/CD-HPG$_{36}$-TAEA$_{30}$ vesicles. (B) *In vitro* DOX·HCl release profiles of C_{18}-AD/CD-HPG$_{36}$-TAEA$_{30}$ nanovesicles at different pH values of 7.4 and 5.0. Data are means ± SD (n = 3).

The release of the drug from the vesicle was investigated at different pH values (Figure 8B). The drug was released in a sustained manner at pH 7.4. Less than 40% of the initial loaded drug was liberated during a long period of 156 h. However, the decline of the solution pH to 5.0 simulating the endosomal pH induced an obvious acceleration of release; more than 80% of the drug was eventually released. Under acid conditions, the cohesion within the vesicle membrane ought to be weakened because of the increased hydrophilicity and strengthened charge repulsion among the protonated amine groups,[46−48] making the vesicle membrane leakier with respect to encapsulated drugs and resulting in accelerated drug release. This pH-dependent characteristic would facilitate the DOX release inside cells upon endocytosis into the acid endosome/lysosome, thus propelling the diffusion of DOX into nucleus for the pharmacological action.

The drug-loaded vesicles were complexed with YOYO-1 iodide-labeled pGL-3 plasmid (green) and then co-incubated with COS7 cells for 8 h. The following CLSM observation offered information about the localization of the condensed plasmid and the entrapped drugs inside cells. The nuclei were stained blue by Hoechst 33342 to distinguish them from the green plasmid and red DOX. As shown in Figure 9, the overlapping of green and red fluorescent spots was evident, suggesting a high degree of colocalization of DNA and the drug. This finding demonstrated the simultaneous coloading and concurrent cellular internalization of drugs and DNAs through the carrier-mediated endocytosis pathway. In addition, it was found that two kinds of payloads can efficiently enter the nucleus domain. This is appealing because both the DOX and therapeutic gene have to be taken up by the nuclei for the effective therapeutic actions.[49,50]

The *in vitro* transfection mediated by the drug-loaded complexes was further performed to study the possible influence of drug inclusion on the transfection performance.[51,52] As shown in Figure 10, regardless of the addition of serum, the transfection efficiencies of the vesicles remained at a comparably high level after the drug had been loaded into the vesicles, suggesting the weak influence of drug loading on transfection.

4. CONCLUSIONS

This work developed a supramolecular amine-rich amphiphile derived from the host−guest interaction between C_{18}-AD and CD-HPG-TAEA. The cationic amphiphile can readily assemble into nanovesicles. The vesicle could condense DNA into nanoscale complexes and mediate the serum-tolerant transfection *in vitro* at a high level even comparable to that of PEI25K while displaying a much lower cytotoxicity. This kind of vesicle can encapsulate the hydrophilic anticancer drug of DOX·HCl and make the drug release behavior sensitive to the acidic pH. CLSM observation indicated that by the aid of the nanovesicle, the loaded DOX·HCl can be efficiently codelivered

DOI: 10.1021/acsami.5b07549
ACS Appl. Mater. Interfaces 2015, 7, 22084−22094

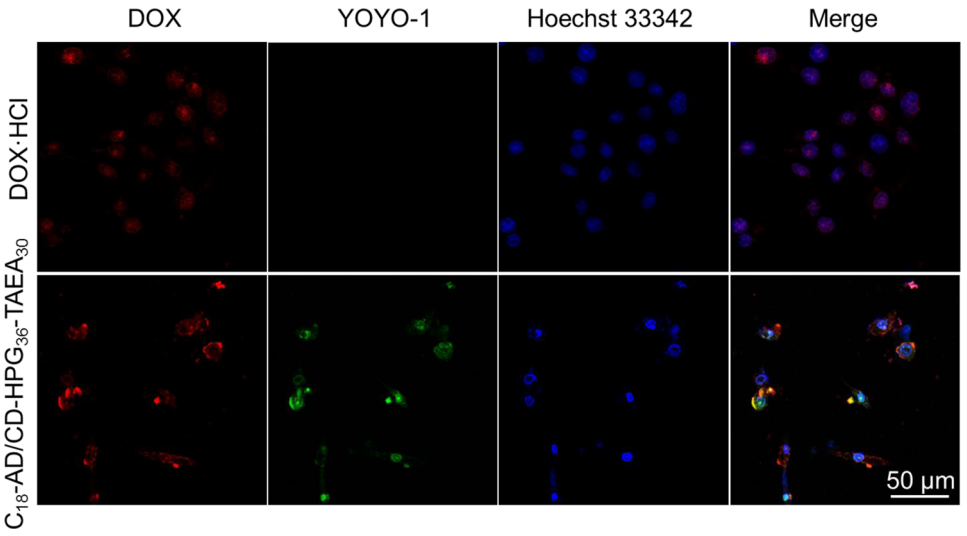

Figure 9. Confocal images of intracellular trafficking of DOX·HCl and DOX·HCl-loaded C_{18}-AD/CD-HPG_{36}-$TAEA_{30}$/DNA complexes prepared at the optimal transfection N/P ratios into COS7 cells for an 8 h co-incubation. Plasmid pGL-3 and nuclei of cells were stained green with YOYO-1 and blue with Hoechst 33342, respectively. The scale bar is 50 μm.

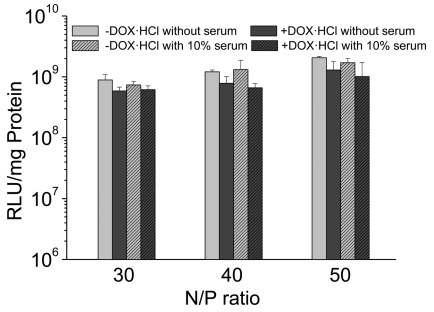

Figure 10. Transfection activities of DOX-loaded and empty C_{18}-AD/CD-HPG_{36}-$TAEA_{30}$ vesicles at various N/P ratios in the absence or presence of 10% serum in COS7 cells. Plasmid pGL-3 was used as the reporter gene. Data are means ± SD (n = 3).

into the cells together with the condensed DNA through the same endocytosis pathway. In addition, the drug loading was found to have little influence on *in vitro* transfection, showing the potential for combinational gene/drug therapy. This paradigm established on the host–guest interaction provides a great chance to extend the functions by partially changing the guest molecules.

AUTHOR INFORMATION

Corresponding Author

*E-mail: fengjun@whu.edu.cn.

Notes

The authors declare no competing financial interest.

ACKNOWLEDGMENTS

This work was financially supported by the National Key Basic Research Program of China (2011CB606202), the National Natural Science Foundation of China (Grants 21374085 and 21174110), the Natural Science Foundation of Hubei Province of China (2014CFB697), and the Fundamental Research Funds for the Central Universities (2042014kf0193).

REFERENCES

(1) Cheng, C. J.; Tietjen, G. T.; Saucier-Sawyer, J. K.; Saltzman, W. M. A Holistic Approach to Targeting Disease with Polymeric Nanoparticles. *Nat. Rev. Drug Discovery* **2015**, *14*, 239–247.

(2) Meng, H.; Mai, W. X.; Zhang, H.; Xue, M.; Xia, T.; Lin, S.; Wang, X.; Zhao, Y.; Ji, Z.; Zink, J. I.; Nel, A. E. Codelivery of an Optimal Drug/siRNA Combination Using Mesoporous Silica Nanoparticles to Overcome Drug Resistance in Breast Cancer in Vitro and in Vivo. *ACS Nano* **2013**, *7*, 994–1005.

(3) Rizzo, L. Y.; Theek, B.; Storm, G.; Kiessling, F.; Lammers, T. Recent Progress in Nanomedicine: Therapeutic, Diagnostic and Theranostic Applications. *Curr. Opin. Biotechnol.* **2013**, *24*, 1159–1166.

(4) Cheng, Y.; Zhao, L.; Li, Y.; Xu, T. Design of Biocompatible Dendrimers for Cancer Diagnosis and Therapy: Current Status and Future Perspectives. *Chem. Soc. Rev.* **2011**, *40*, 2673–2703.

(5) Hu, X.; Liu, G.; Li, Y.; Wang, X.; Liu, S. Cell-Penetrating Hyperbranched Polyprodrug Amphiphiles for Synergistic Reductive Milieu-Triggered Drug Release and Enhanced Magnetic Resonance Signals. *J. Am. Chem. Soc.* **2015**, *137*, 362–368.

(6) Han, K.; Chen, S.; Chen, W. H.; Lei, Q.; Liu, Y.; Zhuo, R. X.; Zhang, X. Z. Synergistic Gene and Drug Tumor Therapy Using a Chimeric Peptide. *Biomaterials* **2013**, *34*, 4680–4689.

(7) Dai, X.; Tan, C. Combination of microRNA Therapeutics with Small-Molecule Anticancer Drugs: Mechanism of Action and Co-Delivery Nanocarriers. *Adv. Drug Delivery Rev.* **2015**, *81*, 184–197.

(8) Creixell, M.; Peppas, N. A. Co-Delivery of siRNA and Therapeutic Agents Using Nanocarriers to Overcome Cancer Resistance. *Nano Today* **2012**, *7*, 367–379.

(9) Gandhi, N. S.; Tekade, R. K.; Chougule, M. B. Nanocarrier Mediated Delivery of siRNA/miRNA in Combination with Chemotherapeutic Agents for Cancer Therapy: Current Progress and Advances. *J. Controlled Release* **2014**, *194*, 238–256.

(10) Ku, S. H.; Kim, K.; Choi, K.; Kim, S. H.; Kwon, I. C. Tumor-Targeting Multifunctional Nanoparticles for siRNA Delivery: Recent Advances in Cancer Therapy. *Adv. Healthcare Mater.* **2014**, *3*, 1182–1193.

(11) Marguet, M.; Bonduelle, C.; Lecommandoux, S. Multicompartmentalized Polymeric Systems: Towards Biomimetic Cellular Structure and Function. *Chem. Soc. Rev.* **2013**, *42*, 512–529.

(12) Kowalczuk, A.; Trzcinska, R.; Trzebicka, B.; Müller, A. H. E.; Dworak, A.; Tsvetanov, C. B. Loading of Polymer Nanocarriers: Factors, Mechanisms and Applications. *Prog. Polym. Sci.* **2014**, *39*, 43–86.

DOI: 10.1021/acsami.5b07549
ACS Appl. Mater. Interfaces 2015, 7, 22084–22094

(13) Hu, Y.; Zhao, N. N.; Yu, B. R.; Liu, F. S.; Xu, F. J. Versatile Types of Polysaccharide-Based Supramolecular Polycation/pDNA Nanoplexes for Gene Delivery. *Nanoscale* **2014**, *6*, 7560−7569.
(14) Zhao, Y.; Yu, B. R.; Hu, H.; Hu, Y.; Zhao, N. N.; Xu, F. J. New Low Molecular Weight Polycation-Based Nanoparticles for Effective Codelivery of pDNA and Drug. *ACS Appl. Mater. Interfaces* **2014**, *6*, 17911−17919.
(15) Li, Y.; Gao, G. H.; Lee, D. S. Stimulus-Sensitive Polymeric Nanoparticles and Their Applications as Drug and Gene Carriers. *Adv. Healthcare Mater.* **2013**, *2*, 388−417.
(16) Discher, D. E.; Eisenberg, A. Polymer Vesicles. *Science* **2002**, *297*, 967−973.
(17) Felber, A. E.; Dufresne, M. H.; Leroux, J. C. pH-Sensitive Vesicles, Polymeric Micelles, and Nanospheres Prepared with Polycarboxylates. *Adv. Drug Delivery Rev.* **2012**, *64*, 979−992.
(18) Fuks, G.; Mayap Talom, R. M.; Gauffre, F. Biohybrid Block Copolymers: Towards Functional Micelles and Vesicles. *Chem. Soc. Rev.* **2011**, *40*, 2475−2493.
(19) Tanner, P.; Baumann, P.; Enea, R.; Onaca, O.; Palivan, C.; Meier, W. Polymeric Vesicles: from Drug Carriers to Nanoreactors and Artificial Organelles. *Acc. Chem. Res.* **2011**, *44*, 1039−1049.
(20) Chen, W.; Meng, F.; Cheng, R.; Zhong, Z. pH-Sensitive Degradable Polymersomes for Triggered Release of Anticancer Drugs: a Comparative Study with Micelles. *J. Controlled Release* **2010**, *142*, 40−46.
(21) Kim, H. K.; Thompson, D. H.; Jang, H. S.; Chung, Y. J.; Van den Bossche, J. pH-Responsive Biodegradable Assemblies Containing Tunable Phenyl-Substituted Vinyl Ethers for Use as Efficient Gene Delivery Vehicles. *ACS Appl. Mater. Interfaces* **2013**, *5*, 5648−5658.
(22) Ren, T. B.; Wu, W.; Jia, M. H.; Dong, H. Q.; Li, Y. Y.; Ou, Z. L. Reduction-Cleavable Polymeric Vesicles with Efficient Glutathione-Mediated Drug Release Behavior for Reversing Drug Resistance. *ACS Appl. Mater. Interfaces* **2013**, *5*, 10721−10730.
(23) Brown, M. D.; Schatzlein, A.; Brownlie, A.; Jack, V.; Wang, W.; Tetley, L.; Gray, A. I.; Uchegbu, I. F. Preliminary Characterization of Novel Amino Acid Based Polymeric Vesicles as Gene and Drug Delivery Agents. *Bioconjugate Chem.* **2000**, *11*, 880−891.
(24) Ding, J.; Xiao, C.; He, C.; Li, M.; Li, D.; Zhuang, X.; Chen, X. Facile Preparation of a Cationic Poly(Amino Acid) Vesicle for Potential Drug and Gene Co-Delivery. *Nanotechnology* **2011**, *22*, 494012.
(25) Chang, Y.; Yang, K.; Wei, P.; Huang, S.; Pei, Y.; Zhao, W.; Pei, Z. Cationic Vesicles Based on Amphiphilic Pillar[5]arene Capped with Ferrocenium: A Redox-Responsive System for Drug/siRNA Co-Delivery. *Angew. Chem., Int. Ed.* **2014**, *53*, 13126−13130.
(26) Mellet, C. O.; Fernandez, J. M. G.; Benito, J. M. Cyclodextrin-Based Gene Delivery Systems. *Chem. Soc. Rev.* **2011**, *40*, 1586−1608.
(27) Chen, G.; Jiang, M. Cyclodextrin-Based Inclusion Complexation Bridging Supramolecular Chemistry and Macromolecular Self-Assembly. *Chem. Soc. Rev.* **2011**, *40*, 2254−2266.
(28) Dass, C. R.; Choong, P. F. Selective Gene Delivery for Cancer Therapy Using Cationic Liposomes: in Vivo Proof of Applicability. *J. Controlled Release* **2006**, *113*, 155−163.
(29) Paleos, C. M.; Tsiourvas, D.; Sideratou, Z.; Pantos, A. Formation of Artificial Multicompartment Vesosome and Dendrosome as Prospected Drug and Gene Delivery Carriers. *J. Controlled Release* **2013**, *170*, 141−152.
(30) Akinc, A.; Thomas, M.; Klibanov, A. M.; Langer, R. Exploring Polyethylenimine-Mediated DNA Transfection and the Proton Sponge Hypothesis. *J. Gene Med.* **2005**, *7*, 657−663.
(31) Storrie, H.; Mooney, D. J. Sustained Delivery of Plasmid DNA from Polymeric Scaffolds for Tissue Engineering. *Adv. Drug Delivery Rev.* **2006**, *58*, 500−514.
(32) Tao, W.; Liu, Y.; Jiang, B.; Yu, S.; Huang, W.; Zhou, Y.; Yan, D. A Linear-Hyperbranched Supramolecular Amphiphile and its Self-Assembly into Vesicles with Great Ductility. *J. Am. Chem. Soc.* **2012**, *134*, 762−764.
(33) Zhao, F.; Yin, H.; Zhang, Z.; Li, J. Folic Acid Modified Cationic Gamma-Cyclodextrin-Oligoethylenimine Star Polymer with Bioreducible Disulfide Linker for Efficient Targeted Gene Delivery. *Biomacromolecules* **2013**, *14*, 476−484.
(34) Yang, B.; Lv, Y.; Wang, Q.; Liu, Y.; An, H.; Feng, J.; Zhang, X.; Zhuo, R. Template-Module Assembly to Prepare Low-Molecular-Weight Gene Transport System with Enhanced Transmembrane Capability. *Sci. China: Chem.* **2014**, *57*, 558−567.
(35) Ding, J.; Xiao, C.; Zhuang, X.; He, C.; Chen, X. Direct Formation of Cationic Polypeptide Vesicle as Potential Carrier for Drug and Gene. *Mater. Lett.* **2012**, *73*, 17−20.
(36) Yang, B.; Sun, Y. X.; Yi, W. J.; Yang, J.; Liu, C. W.; Cheng, H.; Feng, J.; Zhang, X. Z.; Zhuo, R. X. A Linear-Dendritic Cationic Vector for Efficient DNA Grasp and Delivery. *Acta Biomater.* **2012**, *8*, 2121−2132.
(37) Kakizawa, Y.; Kataoka, K. Block Copolymer Micelles for Delivery of Gene and Related Compounds. *Adv. Drug Delivery Rev.* **2002**, *54*, 203−222.
(38) Panyam, J.; Labhasetwar, V. Biodegradable Nanoparticles for Drug and Gene Delivery to Cells and Tissue. *Adv. Drug Delivery Rev.* **2012**, *64*, 61−71.
(39) Xu, F. J.; Yang, W. T. Polymer Vectors via Controlled/Living Radical Polymerization for Gene Delivery. *Prog. Polym. Sci.* **2011**, *36*, 1099−1131.
(40) Erbacher, P.; Zou, S. M.; Bettinger, T.; Steffan, A. M.; Remy, J. S. Chitosan-Based Vector/DNA Complexes for Gene Delivery: Biophysical Characteristics and Transfection Ability. *Pharm. Res.* **1998**, *15*, 1332−1339.
(41) Rinkenauer, A. C.; Schallon, A.; Günther, U.; Wagner, M.; Betthausen, E.; Schubert, U. S.; Schacher, F. H. A Paradigm Change: Efficient Transfection of Human Leukemia Cells by Stimuli-Responsive Multicompartment Micelles. *ACS Nano* **2013**, *7*, 9621−9631.
(42) Luo, X. H.; Huang, F. W.; Qin, S. Y.; Wang, H. F.; Feng, J.; Zhang, X. Z.; Zhuo, R. X. A Strategy to Improve Serum-Tolerant Transfection Activity of Polycation Vectors by Surface Hydroxylation. *Biomaterials* **2011**, *32*, 9925−9939.
(43) Jäger, E.; Jäger, A.; Chytil, P.; Etrych, T.; Rihova, B.; Giacomelli, F. C.; Stepanek, P.; Ulbrich, K. Combination Chemotherapy Using Core-Shell Nanoparticles through the Self-Assembly of HPMA-Based Copolymers and Degradable Polyester. *J. Controlled Release* **2013**, *165*, 153−161.
(44) Du, Y. F.; Chen, W.; Zheng, M.; Meng, F. H.; Zhong, Z. Y. pH-Sensitive Degradable Chimaeric Polymersomes for the Intracellular Release of Doxorubicin Hydrochloride. *Biomaterials* **2012**, *33*, 7291−7299.
(45) Duan, Q.; Cao, Y.; Li, Y.; Hu, X.; Xiao, T.; Lin, C.; Pan, Y.; Wang, L. pH-Responsive Supramolecular Vesicles Based on Water-Soluble Pillar[6]arene and Ferrocene Derivative for Drug Delivery. *J. Am. Chem. Soc.* **2013**, *135*, 10542−10549.
(46) Yang, X.; Grailer, J. J.; Rowland, I. J.; Javadi, A.; Hurley, S. A.; Matson, V. Z.; Steeber, D. A.; Gong, S. Multifunctional Stable and pH-Responsive Polymer Vesicles Formed by Heterofunctional Triblock Copolymer for Targeted Anticancer Drug Delivery and Ultrasensitive MR Imaging. *ACS Nano* **2010**, *4*, 6805−6817.
(47) Song, J.; Zhou, J.; Duan, H. Self-Assembled Plasmonic Vesicles of SERS-Encoded Amphiphilic Gold Nanoparticles for Cancer Cell Targeting and Traceable Intracellular Drug Delivery. *J. Am. Chem. Soc.* **2012**, *134*, 13458−13469.
(48) Madsen, J.; Canton, I.; Warren, N. J.; Themistou, E.; Blanazs, A.; Ustbas, B.; Tian, X.; Pearson, R.; Battaglia, G.; Lewis, A. L.; Armes, S. P. Nile Blue-Based Nanosized pH Sensors for Simultaneous Far-Red and Near-Infrared Live Bioimaging. *J. Am. Chem. Soc.* **2013**, *135*, 14863−14870.
(49) Zhao, F.; Yin, H.; Li, J. Supramolecular Self-Assembly Forming a Multifunctional Synergistic System for Targeted Co-Delivery of Gene and Drug. *Biomaterials* **2014**, *35*, 1050−1062.
(50) Bao, X.; Wang, W.; Wang, C.; Wang, Y.; Zhou, J.; Ding, Y.; Wang, X.; Jin, Y. A Chitosan-Graft-PEI-Candesartan Conjugate for Targeted Co-Delivery of Drug and Gene in Anti-Angiogenesis Cancer Therapy. *Biomaterials* **2014**, *35*, 8450−8466.

DOI: 10.1021/acsami.5b07549
ACS Appl. Mater. Interfaces 2015, 7, 22084−22094

(51) Wang, Y.; Gao, S.; Ye, W. H.; Yoon, H. S.; Yang, Y. Y. Co-Delivery of Drugs and DNA from Cationic Core-Shell Nanoparticles Self-Assembled from a Biodegradable Copolymer. *Nat. Mater.* **2006**, *5*, 791−796.
(52) Yang, B.; Jia, H. Z.; Wang, X. L.; Chen, S.; Feng, J.; Zhang, X. Z.; Zhuo, R. X. Self-Assembled Vehicle Construction via Boronic Acid Coupling and Host-Guest Interaction for Serum-Tolerant DNA Transport and pH-Responsive Drug Delivery. *Adv. Healthcare Mater.* **2014**, *3*, 596−608.

DOI: 10.1021/acsami.5b07549
ACS Appl. Mater. Interfaces 2015, 7, 22084−22094